IEEE Access
Multidisciplinary | Rapid Review | Open Access Journal

Received August 25, 2020, accepted September 7, 2020, date of publication September 24, 2020, date of current version October 2, 2020.

Digital Object Identifier 10.1109/ACCESS.2020.3025897

Particle Swarm Optimization for Interference-Limited Unmanned Aerial Vehicle-Assisted Networks

WENTAO LIU[1,2,3], GUANCHONG NIU[1,2,3], QI CAO[1,3], MAN-ON PUN[1,2,3], (Senior Member, IEEE), AND JUNTING CHEN[1]

[1]School of Science and Engineering, The Chinese University of Hong Kong, Shenzhen 518172, China
[2]Shenzhen Research Institute of Big Data, Shenzhen 518172, China
[3]Shenzhen Key Laboratory of IoT Intelligent Systems and Wireless Network Technology, Shenzhen 518172, China

Corresponding author: Man-On Pun (simonpun@cuhk.edu.cn)

This work was supported in part by the Shenzhen Science and Technology Innovation Committee under Grant ZDSYS20170725140921348 and Grant JCYJ20190813170803617, and in part by the National Natural Science Foundation of China under Grant 61731018.

ABSTRACT This work investigates the deployment of unmanned aerial vehicles (UAVs) as access points to provide wireless services to users in a green field. Three fundamental deployment designs are studied under practical air-to-ground (ATG) channel models, namely the minimum number of UAVs, their optimal deployment locations and the optimal transmit power allocation. Since these three design goals are coupled, a particle swarm optimization (PSO)-based scheme is proposed in conjunction with the balanced Signal to Interference plus Noise Ratio (SINR) transmit power allocation. By exploiting the closed-form expressions of the SINR-balanced optimal power allocation and the resulting SINR, the proposed PSO-based scheme iteratively optimizes the UAV number and subsequently, their locations until the resulting SINR of each user meets its required minimum value. To improve the convergence behavior of the proposed scheme, two schemes are devised to provide an initial estimate on the minimum number of UAVs by analyzing the system sum-rate capacity before using a K-means clustering technique to initialize the UAV locations. Finally, a power fine-tuning scheme is developed to further reduce the total transmit power. Extensive simulation is performed to confirm the good performance of the proposed schemes.

INDEX TERMS Unmanned aerial vehicles, particle swarm optimization, radio resource management.

I. INTRODUCTION

Unmanned aerial vehicles (UAVs) have been envisioned as one of the most promising technologies to revolutionize the future wireless network architectures [1]–[4]. Empowered by their high mobility, UAVs can be deployed as aerial mobile access points or relay nodes in response to real-time data traffic surges. Hence, more comprehensive network coverage can be provided by UAV-assisted networks with flexible network planning and deployment [5]–[14]. For instance, UAV-assisted networks can be deployed as an aerial base station for emergency service recovery when ground communication infrastructure is destroyed by natural disasters such as earthquakes. However, substantial research work is required to realize the benefits promised by UAVs in practice.

First of all, it is critical to optimize the UAV deployment location to improve the UAV's coverage and throughput. In addition to its high dimensionality, the optimization problem incurred in general is non-deterministic polynomial-time hard (NP-hard). In [8], a three-dimensional (3D) air-to-ground (ATG) channel model was established before the optimal altitude is derived as a function of the maximum allowed pathloss and the environment parameters. Based on the ATG channel model, [9] has developed a scheme to determine the 3D locations of low-altitude quadcopter UAVs for joint coverage area and lifetime maximization using the circle packing theory. However, the scheme proposed in [9] assumes non-overlapping coverage, i.e. interference-free environment, which is an issue of concern for realistic

The associate editor coordinating the review of this manuscript and approving it for publication was Nan Wu.

UAV deployment. In the meantime, [11]–[14] proposed heuristic algorithms to optimize the high-altitude UAV deployment. For instance, [13] considered a UAV-assisted heterogeneous network for public safety communications and optimized the UAV deployment by exhaustively searching all feasible deployment locations. In contrast, [12], [14] focused on the single-UAV scenario. More specifically, [12] minimized the total pathloss between the UAV and all users while [14] proposed a dynamic programming approach for UAV trajectory planning by optimizing the UAV's velocity and height. Finally, [17] cast the UAV trajectory design as a mixed-integer non-convex optimization problem to maximize the minimum throughput of all ground users.

Secondly, energy consumption is also a challenging problem for UAV-assisted wireless networks [5], [18]. Since UAVs are battery-driven, they are under very stringent power constraints. For the single-UAV networks, [19] designed schemes to optimize UAV's energy consumption for ground activity detection while [20] investigated UAVs endowed with the energy harvesting capability. In contrast, [18] studied a wireless network equipped with multiple UAVs with emphasis on its energy efficiency and uplink transmission reliability. Furthermore, [18] considered an interference-free scenario by assuming that all UAVs operated in perfectly orthogonal frequency channels. However, the more general interference-*limited* environments were not fully explored in [18]–[20], which can be an issue of concern when multiple UAVs operate in non-orthogonal frequency channels. Clearly, the amount of inter-UAV interference generally increases with the number of UAVs. Thus, it is desirable to deploy the minimum number of UAVs for the benefit of lower cost and better interference management.

In this paper, we focus on the problem of minimizing the number of deployed UAVs based on our previous work [21], while optimizing their deployment locations and transmission power, subject to a minimum SINR value for all users. This task is very challenging as it includes three highly coupled design goals, *i.e.* the minimum number of UAVs, their optimal deployment locations and their optimal transmit power.

To cope with this problem, we propose to jointly optimize the UAV locations and their transmit power while first fixing the number of UAVs. We increase the deployed UAV number if the resulting SINR fails to meet the requirement. This process is repeated until the required SINR is met while the location and transmit power are jointly optimized at each iteration. In sharp contrast to the existing particle swarm optimization (PSO)-based algorithms that used pathloss as the performance measure to direct the UAV location update [12], SINR is explicitly used as the performance measure in evaluating the performance of each UAV location in our algorithms, which enables the proposed scheme to compute the closed-form optimal transmit power and the resulting optimal SINR in a more straightforward manner.

The main contributions of this papers are summarized as follows:

- We develop a computationally efficient PSO-based scheme to jointly optimize the minimum number of UAVs, their deployment locations and their transmit power in an interference-limited UAV-assisted wireless network. To the best of our knowledge, this is the first study to demonstrate such joint optimization is feasible with some simplified assumptions such as perfect knowledge of user locations;
- To further reduce the computational complexity of the proposed PSO-based scheme, we establish a scheme to estimate an initial value for the minimum number of UAVs by analyzing the system sum-rate capacity. Furthermore, a K-means clustering-based scheme is proposed to select the initial UAV positions for the PSO-based scheme intelligently;
- To better preserve the UAV battery power, a sub-optimal power fine-tuning scheme is developed to reduce the total transmit power by carefully reducing the resulting minimum SINR to the targeted minimum SINR.

Notation: Vectors and matrices are denoted by boldface letters. $\boldsymbol{A}^T$ stands for the transpose of matrix $\boldsymbol{A}$ while $\|\boldsymbol{a}\|$ the Euclidean norm of vector $\boldsymbol{a}$. Furthermore, $\boldsymbol{A}_{i,j}$ denotes the i-th row, the j-th column element of $\boldsymbol{A}$ while $(\boldsymbol{A})_k$ the k-th row of the assignment matrix $\boldsymbol{A}$. Finally, a superscript of $(\cdot)^{\mathrm{dB}}$ indicates that the enclosed quantity is in decibel (dB) while quantities without the superscript are real values.

II. REVIEW ON PARTICLE SWARM OPTIMIZATION (PSO)

The Particle Swarm Optimization (PSO) algorithm is one of the most successful intelligent algorithms for solving complex global optimization problems. Inspired by the group behavior of social animals such as bird flocks and fish schools, PSO was first proposed in [22]. It is well-known that these social animals cooperate to increase their access to food through information sharing among the group. This observation has motivated the concept of random agents interacting with each other to search for better solutions cooperatively [22]. Each agent, also known as a particle in PSO, adjusts its search velocity by taking into account its best performance and the best performance of its group. Several improvements on PSO have been proposed. In [23], the original PSO algorithm was enhanced with the introduction of the inertia weight that adjusts the particle velocity generation by generation. It has been shown that a large inertia weight enables the particle to search the optimization space more globally while a smaller inertia weight leads to more local search [23]. Thus, an adaptive inertial weighting strategy is commonly adopted in PSO to improve the particle search. In addition, the shrinkage factor has also been proposed to optimize the multidimensional objective functions. Finally, increasing the number of particles has been shown to improve the performance of PSO at the cost of higher computational complexity.

In the context of UAV deployment optimization, the variables of the PSO algorithm are the possible locations

of UAVs while the optimality of the locations are evaluated by the resulting SINR values of all users. More specifically, the PSO algorithm starts from J initial 3D location vectors, i.e. J particles, denoted by $\boldsymbol{\omega}_j^{(0)}$ of length 3, for $j = 1, 2, \cdots, J$. Then, the PSO scheme updates each of the J location vectors iteratively along the direction leading to improved objective function values. Mathematically, $\boldsymbol{\omega}$ is updated in the following two steps:

$$\begin{aligned} V_j^{(i+1)} &= wV_j^{(i)} + c_1\rho_j(\boldsymbol{\omega}^{(i)*} - \boldsymbol{\omega}^{(i)}) + c_2\phi_j(\boldsymbol{\omega}_g^* - \boldsymbol{\omega}^{(i)}), \\ \boldsymbol{\omega}_j^{(i+1)} &= \boldsymbol{\omega}_j^{(i)} + V_j^{(i+1)}, \end{aligned} \tag{1}$$

where $V_j^{(i)}$ is the velocity at the i-th generation while w is the inertia weight. $\boldsymbol{\omega}^{(i)*}$ and $\boldsymbol{\omega}_g^*$ stand for the locations corresponding to the best performance in the i-th generation and the best particle's location over all iterations so far, respectively. Furthermore, c_1 and c_2 are two learning coefficients that control the influence of local and global components, respectively. Finally, ρ_j and ϕ_j are positive random variables uniformly distributed over [0, 1].

III. SYSTEM MODEL AND PROBLEM FORMULATION

We consider a scenario of deploying K UAVs to serve N single-antenna users in a given field as shown in Fig. 1. In this system, $k \in \mathcal{K} = \{1, 2, \cdots, K\}$ UAVs are deployed to maintain the service for the users. The 3D locations of UAV $k \in \mathcal{K}$ is denoted by $\boldsymbol{\ell}_k = \{x_k^u, y_k^u, h_k^u\}$. Furthermore, we assume that all users are on a horizontal ground with the location of the n-th user being $\boldsymbol{r}_n = \{x_n^r, y_n^r\}$, for $n \in \mathcal{N} = \{1, 2, \cdots, N\}$. Thus, the distance between the k-th UAV and the n-th users is given by

$$d_{k,n} = \sqrt{(x_k^u - x_n^r)^2 + (y_k^u - y_n^r)^2 + (h_k^u)^2}. \tag{2}$$

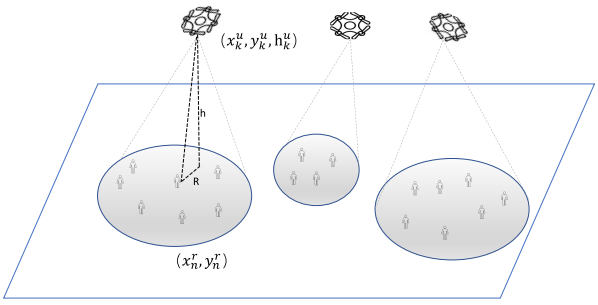

FIGURE 1. Illustration of the deployment scenario.

In this work, we use the low-altitude platforms (LAPs) developed in [8] as the path loss channel model. LAPs are particular suitable for our UAV-assisted emergency communications network in which we assume multiple low-profile and low-altitude UAVs are to be deployed swiftly in the emergency area. A more comprehensive review on the existing UAV communication channel models proposed for various UAV deployment scenarios can be found in [15] and the references therein. Capitalizing on the establishment of a channel model below the stratosphere, LAPs are particularly attractive for applications based on multi-wing UAVs considered in this paper. It is worth noting that small-scale fading effects are *not* considered in the sequel as the main focus of this work is *signal coverage*. Given the assumptions above, the ATG pathloss between the k-th UAV and the n-th user can be written in dB as [8]

$$\mathcal{L}_{k,n}^{\text{dB}} = \frac{\eta_{\text{LoS}} - \eta_{\text{NLoS}}}{1 + ae^{-b(\theta_{k,n}-a)}} + 20\log\left(d_{k,n}\right) + \tau, \tag{3}$$

where

$$\theta_{k,n} = \frac{180}{\pi}\sin^{-1}\left(\frac{h_k^u}{d_{k,n}}\right), \tag{4}$$

$$\tau = 20\log f + 20\log(4\pi/c) + \eta_{\text{NLoS}}, \tag{5}$$

with a, b, η_{LoS}, η_{NLoS} being the environment parameters and $\theta_{k,n}$ the elevation angle. Furthermore, f is the transmitted radio frequency and c is the speed of light.

Assuming that each user can only attach to one UAV, we model the user-UAV association with the following function:

$$\mathcal{A}(n) = k, \tag{6}$$

with $n \in \mathcal{N}$ and $k \in \mathcal{K}$.

Let $\boldsymbol{p}$ be the power allocation strategy $\boldsymbol{p} = [p_1, p_2, \cdots, p_N]^T$ with each element p_n being the transmit power of the n-th user where $n \in \mathcal{N}$. Then, the SINR of the n-th user is given as follows:

$$\Gamma_n = \frac{p_n \cdot \mathcal{L}_{\mathcal{A}(n),n}^{-1}}{I_n + \sigma^2}, \tag{7}$$

where $\mathcal{L}_{k,n} = 10^{\frac{\mathcal{L}_{k,n}^{\text{dB}}}{10}}$. Furthermore, I_n is the total interference that the n-th user receives from all UAVs and given by

$$I_n = \sum_{\substack{m=1 \\ m\neq n}}^{N} \alpha_{\mathcal{A}(m),n} \cdot \frac{p_m}{\mathcal{L}_{\mathcal{A}(m),n}}, \tag{8}$$

with $\alpha_{\mathcal{A}(m),n}$ being the damping factor between the $\mathcal{A}(m)$-th UAV and the n-th user arisen from the non-orthogonality between communication channels [24]. In addition, σ^2 is the thermal noise power of the user.

Finally, we assume that each user is assigned to the UAV with the smallest path loss calculated from the ATG model. We denote by $\mathbf{A}$ the user-UAVs association matrix and define its element as

$$A_{k,n} = \begin{cases} 1 & \text{if } \mathcal{A}(n) = k, \\ 0 & \text{otherwise}, \end{cases} \tag{9}$$

for $k \in \mathcal{K}$ and $n \in \mathcal{N}$.

Now, we present our UAV deployment problem to jointly optimize the number of deployed UAVs, their locations, and

their transmit power, subject to the SINR requirement for each user. It can be written as

$$\mathcal{P}1: \min_{\boldsymbol{p},\{\boldsymbol{\ell}_k\}} \quad K \tag{10}$$

$$\text{Subject to}: \min_{n\in\mathcal{N}} \Gamma_n \geq \Gamma_0, \tag{C_1}$$

$$\sum_n A_{k,n}\cdot p_n \leq P_{k,\max}, \quad \forall k \in \mathcal{K} \tag{C_2}$$

$$\boldsymbol{\ell}_k \in \mathcal{D}, \quad \forall k \in \mathcal{K} \tag{C_3}$$

$$||\boldsymbol{\ell}_j - \boldsymbol{\ell}_k||_2 \geq d_s, \quad \forall j,k \in \mathcal{K} \tag{C_4}$$

$$\sum_k A_{k,n} = 1, \quad \forall n \in \mathcal{N} \tag{C_5}$$

where $P_{k,\max}$ is the maximum transmit power of the k-th UAV, d_s is the safety distance. Furthermore, Γ_0 and $\mathcal{D}$ are the minimum required SINR and the set of feasible UAV locations, respectively.

In the first constraint C_1 of the optimization problem above, Γ_0 is the SINR requirement that all users must achieve. It represents the SINR constraint. In the second constraint C_2, it shows the maximum transmission power $P_{k,\max}$ for each UAV as the power constraints. In the third constraint C_3, the locations of UAVs must reside in the feasible area set. The constraint C_4 aims to prevent any two UAVs from hovering in the same 3D location, which effectively avoids UAV collision. It should be pointed out that the UAV collision mentioned above is different from the collision caused by two UAVs' flight trajectories intersecting each other. Finally, C_5 requires that each user can only be attached to one UAV.

Clearly, the optimization problem in (10) is non-convex in the high-dimensional space. Therefore, it is difficult to analytically find its optimal solution. In the following, we propose a highly computationally efficient scheme as shown in Fig. 2, which leads to a sub-optimal solution to (10).

IV. PROPOSED PSO-BASED DEPLOYMENT SCHEME

Our approach is inspired by the following intuition: Starting from K_{init} UAVs, a joint optimization on the UAV positioning and transmit power is performed according to (10); If any of the resulting SINR fails to meet the required Γ_0, we then increase the number of UAVs by one; This process is repeated until the minimum SINR of all users exceeds or is equal to Γ_0; When the process is terminated, the minimum number of deployed UAVs K^* is also found. In practice, a computation center in the emergency area will first collect all user locations before running the proposed PSO-based scheme offline to design the number of required UAVs as well as their 3D hovering locations and transmit power allocated to each user.

Clearly, if K^* is the minimum number of UAVs, then K^* iterations are required for the proposed scheme initialized with $K_{init} = 1$. Thus, it is highly desirable to have a more accurate K_{init} to reduce the number of PSO iterations. In Sec. IV-B, a more accurate K_{init} is generated by approximating the sum-rate downlink capacity of the multi-UAV network.

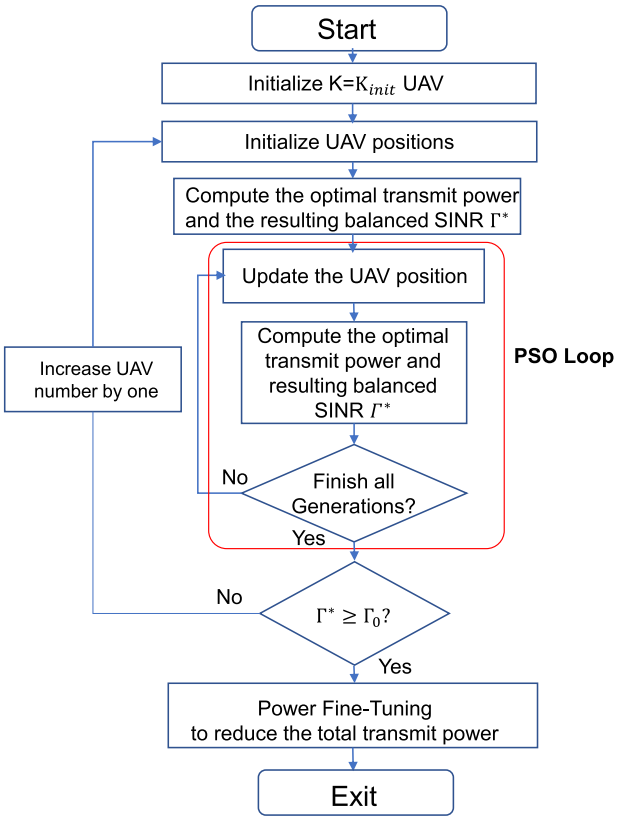

FIGURE 2. Flowchart of the proposed PSO-based scheme.

A. PSO-BASED DEPLOYMENT SCHEME

To cope with the high-dimensional searching space for the optimal UAV locations, we propose a PSO-based scheme. More specifically, the PSO algorithm utilizes a population of particles each of which represents a UAV location vector. Then, each particle's movement is influenced by its local best known position as well as its best known positions that are updated by other better performing particles over all existing iterations.

1) K-MEANS CLUSTERING INITIALIZATION

It is well-known that good initialization of the first-generation particles is vital for the PSO algorithm. In contrast to random initialization, an initialization method based on the K-means clustering technique is proposed to generate the horizontal positions of the first-generation particles. More specifically, the proposed initialization method groups N users into K clusters by minimizing the following error.

$$\epsilon = \sum_{k=1}^{K}\sum_{n=1}^{N} \delta_{k,n} \left\|\boldsymbol{r}_n - \boldsymbol{s}_k\right\|^2, \tag{11}$$

where $\boldsymbol{s}_k$ is the centroid of the k-th cluster on the ground (also used as the horizontal location of the k-th UAV) and

$$\delta_{k,n} = \begin{cases} 1 & n \in \mathcal{C}_k, \\ 0 & \text{otherwise}, \end{cases} \tag{12}$$

with $\mathcal{C}_k$ being the user index set for all users grouped into the k-th cluster, for $k = 1, 2, \cdots, K$.

Recalling that $\{\boldsymbol{s}_k\}$ only contains (x, y), we will have to append a randomly generated height to each $\boldsymbol{s}_k$ to produce $\tilde{\boldsymbol{s}}_k$. Then, we initialize

$$\boldsymbol{\omega}_j^{(0)} = \left[\tilde{\boldsymbol{s}}_1^T, \tilde{\boldsymbol{s}}_2^T, \cdots, \tilde{\boldsymbol{s}}_K^T\right]^T, \tag{13}$$

for $j = 1, 2, \cdots, J$.

Finally, the above K-means clustering iteration is repeated for J times before J sets of $\boldsymbol{\omega}_j^{(0)}$ are obtained as the initial positions for the first-generation UAV locations to be input into the proposed PSO-based scheme. In the sequel, the PSO-based scheme with the K-means clustering initialization is referred to as PSO-KMeans while the random initialization is referred to as PSO-Rand.

2) PSO-BASED UAV LOCATION OPTIMIZATION

In the proposed PSO-scheme, it starts from the first-generation location vectors $\boldsymbol{\omega}_j^{(0)}$, for $j = 1, 2, \cdots, J$, as the initial UAV locations. Then it iteratively updates each of the J position vectors in the direction that leads to improved SINR values. For each position vector in its i-th generation, the proposed scheme implements an SINR balanced power control algorithm to optimize the transmission power allocated to each user. More information on the transmit power control algorithm will be provided in the next section.

In sharp contrast to [12] in which the PSO algorithm is used to minimize the total pathloss from one single UAV to all users by optimizing the UAV location, we consider optimizing the locations of multiple UAVs to improve the users' SINR values. We denote by $\boldsymbol{\omega}$ the UAV location vector of K UAVs as

$$\boldsymbol{\omega} = \left[\boldsymbol{\ell}_1^T, \boldsymbol{\ell}_2^T, \cdots, \boldsymbol{\ell}_K^T\right]^T. \tag{14}$$

Then, the proposed scheme updates each of the J location vectors iteratively along the direction leading to improved user SINR. More specifically, let $\boldsymbol{\omega}^{(i)*}$ and $\boldsymbol{\omega}_g^*$ stand for the location vector corresponding to the best SINR in the i-th generation and over all generations, respectively. After obtaining the resulting SINR for each location vector $\boldsymbol{\omega}_j^{(i)}$ in the i-th generation, the proposed PSO algorithm then ranks all J location vectors, for $j = 1, 2, \cdots, J$, based upon their corresponding SINR values before updating $\boldsymbol{\omega}^{(i)*}$ and $\boldsymbol{\omega}_g^*$.

3) SINR-BALANCED POWER ALLOCATION ALGORITHM

In this part, we elaborate on the transmit power allocation algorithm for a given set of UAV locations. Most existing power allocation algorithms are computationally expensive, which renders them impractical as the PSO scheme iteratively updates the UAV locations generation by generation. Rather than directly minimizing the total transmit power, we propose to focus on the transmit power allocation to achieve an identical SINR (also known as balanced SINR) for all users by exploiting the balanced SINR method proposed in [25]. The advantage of the proposed approach is that the transmit power and the resulting SINR can be derived analytically by solving the following equation.

$$\frac{1}{\Gamma_n} \cdot p_n = \sum_{\substack{m=1 \\ m \neq n}}^{N} \alpha_{\mathcal{A}(m),n} \cdot \frac{\mathcal{L}_{\mathcal{A}(n),n}}{\mathcal{L}_{\mathcal{A}(m),n}} \cdot p_m + \sigma^2 \cdot \mathcal{L}_{\mathcal{A}(n),n}. \tag{15}$$

To solve (15), we first define $\boldsymbol{G} \in \mathbb{C}^{N \times N}$ as:

$$G_{n,m} = \begin{cases} \alpha_{\mathcal{A}(m),n} \cdot \dfrac{\mathcal{L}_{\mathcal{A}(n),n}}{\mathcal{L}_{\mathcal{A}(m),n}} & \text{if } n \neq m, \\ 0 & \text{otherwise,} \end{cases} \tag{16}$$

for $n, m \in \mathcal{N}$.

If we set the target SINR the same for all users, *i.e.* balanced SINR $\Gamma_n = \Gamma$ for $n \in \mathcal{N}$, then (15) can be rewritten in the following matrix form [25]:

$$\frac{1}{\Gamma} \cdot \begin{bmatrix} p_1 & p_2 & \cdots & p_N & 0 \end{bmatrix}^T = \boldsymbol{B} \cdot \boldsymbol{y}, \tag{17}$$

where we define

$$\boldsymbol{y} = [p_1, p_2, \cdots p_N, 1]^T, \tag{18}$$

and

$$\boldsymbol{B} = \begin{bmatrix} \boldsymbol{G} & \boldsymbol{h}_{N\times 1} \\ \boldsymbol{0}_{1\times N} & 0 \end{bmatrix}, \tag{19}$$

with

$$\boldsymbol{h} = \sigma^2 \cdot \left[\mathcal{L}_{\mathcal{A}(1),1}, \mathcal{L}_{\mathcal{A}(2),2}, \cdots \mathcal{L}_{\mathcal{A}(N),N}\right]^T. \tag{20}$$

Next, we define matrix $\boldsymbol{C}$ of size $(N+1) \times (N+1)$ as

$$\boldsymbol{C} = \begin{bmatrix} \boldsymbol{I}_{N\times N} & \boldsymbol{0}_{N\times 1} \\ (\boldsymbol{A})_k & -P_{k,\max} \end{bmatrix}, \tag{21}$$

where $(\boldsymbol{A})_k$ is the k-th row of the user-UAV association matrix $\boldsymbol{A}$ defined in (9).

Since $\boldsymbol{C}$ is a lower triangular matrix, $\boldsymbol{C}^{-1}$ can be found in a straightforward manner as

$$\boldsymbol{C}^{-1} = \begin{bmatrix} \boldsymbol{I}_{N\times N} & \boldsymbol{0}_{N\times 1} \\ -\dfrac{(\boldsymbol{A})_k \cdot \boldsymbol{I}_{N\times N}}{P_{k,\max}} & -\dfrac{1}{P_{k,\max}} \end{bmatrix}. \tag{22}$$

Pre-multiplying $\boldsymbol{C}^{-1}$ on both sides of (17), we have

$$\frac{1}{\Gamma} \cdot \underbrace{\boldsymbol{C}^{-1} \begin{bmatrix} p_1 & p_2 & \cdots & p_N & 0 \end{bmatrix}^T}_{\boldsymbol{y}} = \underbrace{\boldsymbol{C}^{-1} \cdot \boldsymbol{B}}_{\boldsymbol{D}} \boldsymbol{y}, \tag{23}$$

$$\frac{1}{\Gamma} \cdot \boldsymbol{y} = \boldsymbol{D} \cdot \boldsymbol{y}, \tag{24}$$

where

$$\boldsymbol{D} = \boldsymbol{C}^{-1} \cdot \boldsymbol{B} = \begin{bmatrix} \boldsymbol{G} & \boldsymbol{h}_{N\times 1} \\ \dfrac{(\boldsymbol{A})_k \cdot \boldsymbol{G}}{P_{k,\max}} & \dfrac{(\boldsymbol{A})_k \cdot \boldsymbol{h}}{P_{k,\max}} \end{bmatrix}. \tag{25}$$

Inspection of (24) suggests that the optimal power allocation vector $\boldsymbol{y}^*$ is given by the eigenvector of $\boldsymbol{D}$ corresponding to the largest eigenvalue λ^* with the resulting SINR shown below [25]

$$\Gamma^* = \frac{1}{\lambda^*}. \tag{26}$$

In our proposed PSO-based scheme, Γ^* is then employed to direct the UAV location updates in each generation. If Γ^* dervied from multiple PSO generations cannot meet the target value Γ_0, then the PSO-based scheme determines that the current number of UAVs is insufficient. Subsequently, the proposed scheme will be repeated after one more UAV is added to provide services. In contrast, for the case of $\Gamma^* \geq \Gamma_0$, the PSO-based scheme will be terminated before further power fine-tuning proposed in the next section is performed.

4) POWER FINE-TUNING

It should be pointed out that Γ^* is achieved above Γ_0, i.e. $\Gamma^* \geq \Gamma_0$, by allowing each UAV to transmit at its maximum transmit power. Motivated by this observation, we can perform fine adjustments on the UAV transmit power to make the resulting SINR barely exceed the target SINR. In this section, we would like to find the sub-optimal $\boldsymbol{y}$ that satisfies $\Gamma^* \geq \Gamma_0$ and has the smallest total transmit power. This problem can be reformulated as searching for a scaling factor β:

$$\begin{aligned} \mathcal{P}2: \ \min \quad & \beta && (27)\\ \text{Subject to}: \ & \min_{n\in\mathcal{N}} \Gamma_n \geq \Gamma_0, && (C_1)\\ & \sum_n A_{k,n}\cdot p_n \leq \beta P_{k,\max}, \quad \forall k \in \mathcal{K}, && (C_2)\\ & 0 < \beta \leq 1. && (C_3) \end{aligned}$$

Clearly, the minimum β^* is restricted by the UAV that has the tightest transmit power constraint. Assuming that the k-th UAV transmits at its maximum power, we have

$$\sum_n A_{k,n} \cdot p_n = \beta^* \cdot P_{k,\max}.$$

Using (17)-(25), it is straightforward to show that the new matrix $\boldsymbol{D}'$ is given by

$$\boldsymbol{D}' = \begin{bmatrix} \boldsymbol{G} & \boldsymbol{h}_{N\times 1} \\ \dfrac{(\boldsymbol{A})_k \cdot \boldsymbol{G}}{\beta^* \cdot P_{k,\max}} & \dfrac{(\boldsymbol{A})_k \cdot \boldsymbol{h}}{\beta^* \cdot P_{k,\max}} \end{bmatrix}. \tag{28}$$

As a result, $\mathcal{P}2$ in (27) is simplified to the derivation of the largest eigenvalue of $\boldsymbol{D}'$. Since $0 < \beta \leq 1$, we propose to use exhaustive search to find β^*. Starting from $\beta = 1 - \Delta\beta$ where $\Delta\beta$ is a pre-defined step size, we can repeatedly reduce the current β value by $\Delta\beta$ until the largest eigenvalue of $\boldsymbol{D}'$ is less than Γ_0. Then, we can find β^* equal to the sum of the current β value and $\Delta\beta$.

5) COMPLEXITY ANALYSIS

As discussed above, the proposed algorithm first employs the PSO algorithm to iteratively optimize the resulting balanced SINR, transmit power as well as the UAV locations. For a given number of UAVs, the computational complexity of this process per generation is estimated as $\mathcal{O}\left(J \cdot i_{totol} \cdot N^3\right)$, where N is the number of users, J is the total number of particles and i_{totol} is the total number of PSO generations. Furthermore, assuming the worst case in which the PSO algorithm starts from $K_{init} = 1$, K iterations are performed. Thus, the total computational complexity is given by $\mathcal{O}\left(K \cdot J \cdot i_{totol} \cdot N^3\right)$. In addition, the power fine-tuning requires computation of $\mathcal{O}\left(\frac{1-\beta^*}{\Delta\beta} \cdot N^3\right)$. Therefore, the total computational complexity of the proposed PSO-based scheme is given by $\mathcal{O}\left(K \cdot J \cdot i_{totol} \cdot N^3 + \frac{1-\beta^*}{\Delta\beta} \cdot N^3\right)$.

B. INITIALIZATION OF K

As shown in the complexity analysis above, K^* PSO iterations are required if the proposed PSO-based scheme initializes $K_{\text{init}} = 1$, where K^* is the minimum number of UAVs that can provide an SINR larger than or equal to Γ_0 to all users. To reduce the computational complexity, it is desirable to have a more accurate K_{init}. In this section, we will derive a more accurate initial value for K by approximating the sum-rate downlink capacity of a multi-UAV network.

Since the minimum SINR Γ_0 is required for each of the N users, the minimum total data rate required can be expressed as

$$C_{\text{req}} = N \cdot \log(1 + \Gamma_0). \tag{29}$$

Clearly, the sum-rate capacity of the resulting K-UAV network has to be larger than C_{req}. In principle, if the sum-rate capacity of any K-UAV networks could be derived as a function of K, we could easily find an appropriate initial value for K. Unfortunately, the sum-rate capacity of a multi-UAV network remains an open research question. In the sequel, we will first analyze the sum-rate capacity provided by a single-UAV network before proposing a heuristic scheme to estimate a more accurate K_{init}. As a result, the improved K_{init} will help reduce the PSO iterations and subsequently, the total computational complexity.

1) SUM-RATE FOR SINGLE-UAV NETWORKS

We begin with a network comprised of one UAV and N users. The sum-rate capacity of such a single-UAV network can be expressed as a function of N in the following form:

$$\begin{aligned} & C_{\text{SingleUAV}}(N) \\ &= \sum_{n=1}^{N} \log\left(1 + \Gamma_n\right) \\ &= \sum_{n=1}^{N} \log \left\{ \frac{\sum_{m=1}^{N} \alpha_{m,n} \cdot \dfrac{p_m \mathcal{L}_{\mathcal{A}(n),n}}{\mathcal{L}_{\mathcal{A}(m),n}} + \Psi_n \cdot \mathcal{L}_{\mathcal{A}(n),n}}{\sum_{\substack{m=1 \\ m\neq n}}^{N} \alpha_{m,n} \cdot \dfrac{p_m \mathcal{L}_{\mathcal{A}(n),n}}{\mathcal{L}_{\mathcal{A}(m),n}} + \Psi_n \cdot \mathcal{L}_{\mathcal{A}(n),n}} \right\} \\ &= \sum_{n=1}^{N} \log \frac{[(\boldsymbol{G} + \boldsymbol{I}) \cdot \boldsymbol{p}]_n + \boldsymbol{h}_n}{[\boldsymbol{G} \cdot \boldsymbol{p}]_n + \boldsymbol{h}_n}, \end{aligned} \tag{30}$$

where $[\cdot]_n$ denotes the n-th element of the enclosed vector.

Thus, the problem of finding the maximum sum rate of a single UAV network can be written as follows:

$$\mathcal{P}3: \max_{\boldsymbol{p}} \sum_{n=1}^{N} \log \frac{[(\boldsymbol{G}+\boldsymbol{I})\cdot\boldsymbol{p}]_n + [\boldsymbol{h}]_n}{[\boldsymbol{G}\cdot\boldsymbol{p}]_n + [\boldsymbol{h}]_n} \tag{31}$$

$$\text{Subject to}: \sum_{n=1}^{N} p_n \le P_{1,\max}, \tag{C_1}$$

$$p_n \ge 0, \quad \forall\, n \in \mathcal{N}. \tag{C_2}$$

Clearly, $\mathcal{P}3$ is a non-convex and non-trivial optimization problem. Following the approach developed in [26], we will develop a heuristic method to solve $\mathcal{P}3$ via the successive convex approximation. We begin with defining $\boldsymbol{F}$ as [26]

$$\boldsymbol{F} = \boldsymbol{G} + \frac{1}{P_{1,\max}} \cdot \boldsymbol{h} \cdot \mathbf{1}^T. \tag{32}$$

After some straightforward algebraic manipulations, we can rewrite $\mathcal{P}3$ as

$$\mathcal{P}4: \min_{\boldsymbol{p}} \prod_{n=1}^{N} \frac{[\boldsymbol{F}\cdot\boldsymbol{p}]_n}{[(\boldsymbol{F}+\boldsymbol{I})\cdot\boldsymbol{p}]_n} \tag{33}$$

$$\text{Subject to}: \sum_{n=1}^{N} p_n \le P_{1,\max}, \tag{C_1}$$

$$p_n \ge 0, \quad \forall\, n \in \mathcal{N}, \tag{C_2}$$

Recalling (16), we have $G_{n,m} \ge 0$ for $n, m \in \mathcal{N}$, i.e. each element of $\boldsymbol{G}$ is non-negative. Thus, it is straightforward to show that $\boldsymbol{F}$ defined in (32) is a non-negative matrix by exploiting the fact that each entry of $\boldsymbol{h}$ defined in (20) is non-negative. As shown in [27], there exists a quasi-inverse of a nonnegative square matrix denoted by $\widetilde{\boldsymbol{F}}$ for the nonnegative square matrix $\boldsymbol{F}$ with the following properties:

$$(\boldsymbol{I}+\boldsymbol{F})(\boldsymbol{I}-\widetilde{\boldsymbol{F}}) = \boldsymbol{I}, \tag{34}$$

$$\widetilde{\boldsymbol{F}}(\boldsymbol{I}+\boldsymbol{F}) = \boldsymbol{F}. \tag{35}$$

Next, we define

$$\boldsymbol{z} = (\boldsymbol{I}+\boldsymbol{F})\cdot\boldsymbol{p}, \tag{36}$$

$$\boldsymbol{\xi} = \log \boldsymbol{z}. \tag{37}$$

Using (35)-(37), we can show that

$$\boldsymbol{F}\cdot\boldsymbol{p} = \left[\widetilde{\boldsymbol{F}}(\boldsymbol{I}+\boldsymbol{F})\right]\cdot\boldsymbol{p} = \widetilde{\boldsymbol{F}}\cdot\boldsymbol{z} = \widetilde{\boldsymbol{F}}\cdot e^{\boldsymbol{\xi}}. \tag{38}$$

Furthermore, since $\boldsymbol{I}+\boldsymbol{F}$ is non-singular, (36) can be rewritten as

$$\boldsymbol{p} = (\boldsymbol{I}+\boldsymbol{F})^{-1}\boldsymbol{z} = (\boldsymbol{I}-\widetilde{\boldsymbol{F}})\cdot e^{\boldsymbol{\xi}}, \tag{39}$$

where the last equality is derived from (34) and (37).

Finally, $\mathcal{P}4$ can be transformed into a convex optimization by utilizing (36) and (38).

$$\mathcal{P}5: \min_{\boldsymbol{\xi}} \prod_{n=1}^{N} \frac{\left[\widetilde{\boldsymbol{F}}\cdot e^{\boldsymbol{\xi}}\right]_n}{\left[e^{\boldsymbol{\xi}}\right]_n} \tag{40}$$

$$\text{Subject to}: \mathbf{1}^T(\boldsymbol{I}-\widetilde{\boldsymbol{F}})\cdot e^{\boldsymbol{\xi}} \le P_{1,\max}, \tag{C_1}$$

$$\text{Subject to}: \frac{\left[\widetilde{\boldsymbol{F}}\cdot e^{\boldsymbol{\xi}}\right]_n}{\left[e^{\boldsymbol{\xi}}\right]_n} \le 1, \quad \forall n. \tag{C_2}$$

Since $\mathcal{P}5$ has the same form as those problems shown in [26]–[28], we can solve $\mathcal{P}5$ using the same approach developed in [26]–[28] and derive $C_{\text{SingleUAV}}$ for any given $\boldsymbol{F}$.

2) SUM-RATE FOR MULTI-UAV NETWORKS

Next, we consider an interference-limited network comprised of K UAVs and N users with each user being served by only one UAV. Denote by C_k and r_n the sum-rate capacity of the k-th UAV and the required data rate for the n-th user, respectively. To support all N users, the sum-rate capacity of such a K-UAV network must satisfy the following inequality:

$$\sum_{k=1}^{K} C_k \ge C_{\text{req}}. \tag{41}$$

We can approximate (41) as follows:

$$\sum_{k=1}^{K} C_k \approx K \times C_{\text{SingleUAV}}(N) \ge C_{\text{req}}, \tag{42}$$

or

$$K \ge \frac{C_{\text{req}}}{C_{\text{SingleUAV}}(N)}. \tag{43}$$

Thus, we can initialize K as

$$K_{\text{init}} = \frac{C_{\text{req}}}{C_{\text{SingleUAV}}(N)}. \tag{44}$$

Since $C_{\text{SingleUAV}}(N)$ is a function of N, the initial value of K can be alternatively found by solving the following fixed-point equation derived from (44).

$$K_{\text{init}} = \frac{C_{\text{req}}}{C_{\text{SingleUAV}}\left(\frac{N}{K_{\text{init}}}\right)}. \tag{45}$$

In the sequel, the initialization schemes in (44) and (45) are referred to as "Init.K LBND" and "Init.K FixedPt", respectively.

V. SIMULATION RESULTS

In this section, we will conduct extensive simulation to confirm the performance of the proposed PSO-based scheme. In our simulation, N users are randomly and evenly distributed within a geographic area of size 500×500 m^2. As suggested in [15], [16], the radius of the service area of the low-altitude UAVs is on the order of magnitude of 100 meters. Each UAV has a maximum transmit power of $P_{\max} = 100$ mW, *i.e.* 20 dBm. While the UAV height is limited to be within [10, 100] meters. Furthermore, the ATG models corresponding to the urban environment are used in modeling the pathloss with $a = 9.60$, $b = 0.16$, $\eta_{LoS} = 1.0$ and $\eta_{NLoS} = 20$. Finally, the intra-cell and inter-cell damping factors α_0 and α_1 are set as 0.01 and 10^{-4}, respectively. Unless specified otherwise, we set $\sigma^2 = 10^{-10}$ mW and the target SINR value Γ_0^{dB} equal to 0 dB in the following

experiments. Clearly, the proposed scheme is applicable to systems of any practical Γ_0^{dB} values.

Fig. 3 shows the balanced SINR value (in dB) of the proposed PSO-based scheme with the PSO-Kmeans initialization, where the deployed UAV number K is set to be 3, 4 and 5. When a few users are scattered in the given area, *i.e.* $N \leq 50$, three UAVs can cover all users, and the SINR of each user is higher than 0 dB. However, as the number of users increases from 51 to 65, the final balanced SINR gradually decreases to 0 dB. This is because the interference grows as more users share the same spectrum and a fixed maximum transmit power $P_{k,\max}$. When N increases above 50, four UAVs are required to provide the target SINR of 0 dB to all users. Similarly, for $N \geq 65$, as shown by the yellow curve on the far right, five UAVs are required.

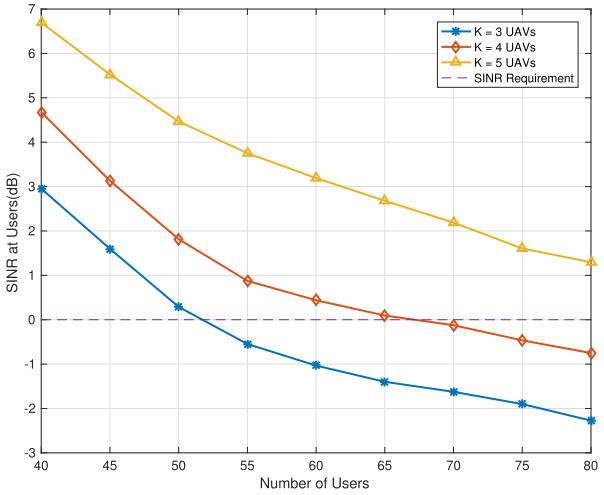

FIGURE 3. Achievable balanced SINR performance as a function of user and UAV numbers.

Fig. 4 shows the PSO algorithm iteratively updates the 3D locations of $K = 3$ UAVs based on the particle swarm optimization. Examination of Fig. 4 shows that the UAV's position converges quickly only after a few generations.

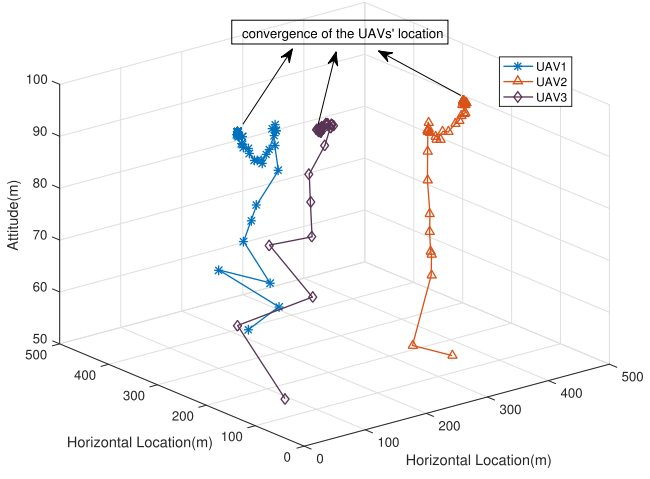

FIGURE 4. PSO updates of UAV 3D locations for $K = 3$ UAVs.

Next, we compare the performance of PSO-Rand and PSO-KMeans with $K = 5$. Fig. 5 shows the average SINR achieved by PSO KMeans and PSO-Rand over 200 runs. First, the curve labelled as "KMeans only" shows the performance of positioning the UAVs at the cluster centroids derived from the standard K-means clustering technique. Fig. 5 indicates that both the PSO-based algorithms, namely PSO-Rand and PSO-KMeans, outperform "KMeans only", which indicates that the cluster centroids derived from the standard K-means clustering technique without PSO iterations are not proper UAV deployment locations. Finally, investigation of Fig. 5 shows that PSO-KMeans outperforms PSO-Rand over all user numbers tested, which confirms that the K-means clustering method provides better initial points leading to higher balanced SINR values.

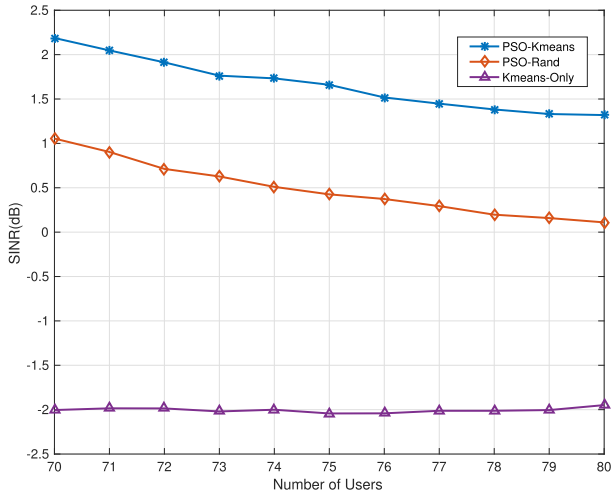

FIGURE 5. SINR performance comparison as a function of users for $K = 5$ UAVs.

Fig. 6 shows the SINR convergence behavior as a function of generations with $K = 5$ and $N = 80$. While PSO-KMeans outperforms PSO-Rand in terms of the achievable balanced SINR, Fig. 6 suggests that their convergence behavior is very similar.

Next, we set $K = 3$ and $\Delta\beta = 0.01$ to evaluate the performance of the proposed power fine-tuning algorithm. Fig. 7 shows the total power sent to all users, *i.e.* $\sum_{n=1}^{N} p_n$, as a function of the total number of users. In Fig. 7, the blue curve with asterisk markers and the red curve with triangle markers stand for the total power with and without the proposed power fine-tuning algorithm, respectively. Clearly, Fig. 7 shows that the power fine-tuning process significantly improves the power efficiency, especially when N is small. This result can also be confirmed from Fig. 3 where the SINR achieved by PSO KMeans is about $\Gamma^{*\text{dB}} = 3$ dB for $K = 3$ and $N = 40$. Therefore, the transmission power can be further optimized while keeping the SINR of all users barely higher than $\Gamma_0^{\text{dB}} = 0$ dB.

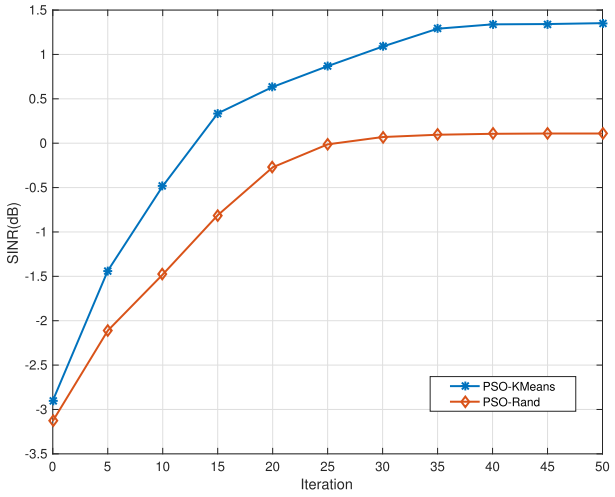

FIGURE 6. Convergence behavior as a function of the PSO generation number.

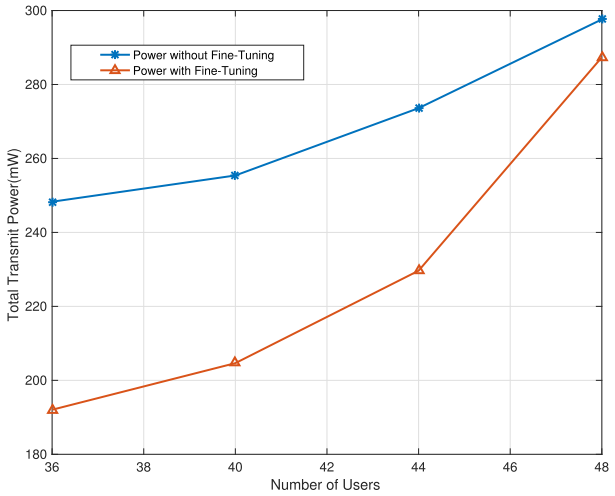

FIGURE 7. Total transmit power as a function of users for $K = 3$ UAVs.

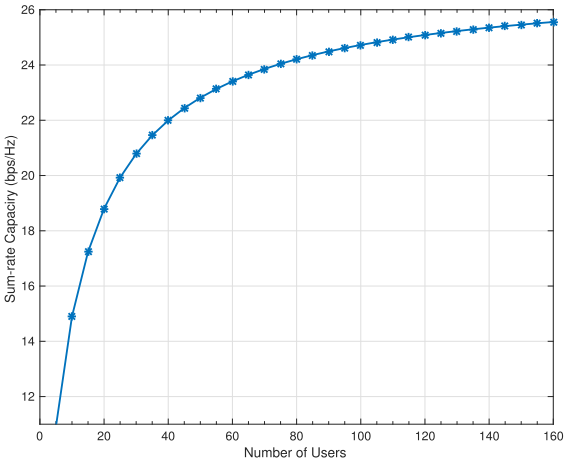

FIGURE 8. The single-UAV sum-rate capacity as a function of user numbers N.

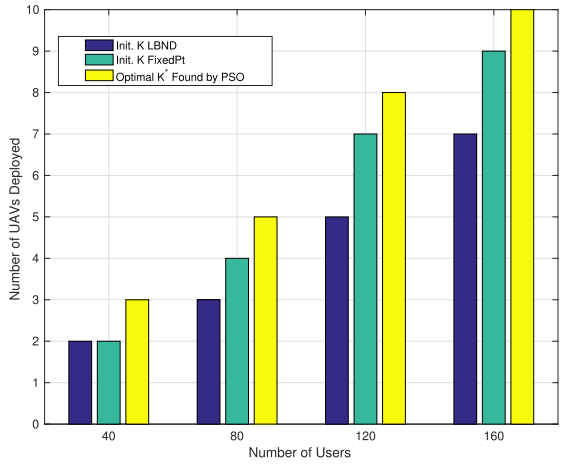

FIGURE 9. Initial K values estimated by the two proposed initialization schemes as compared to the optimal K^* found by the PSO scheme.

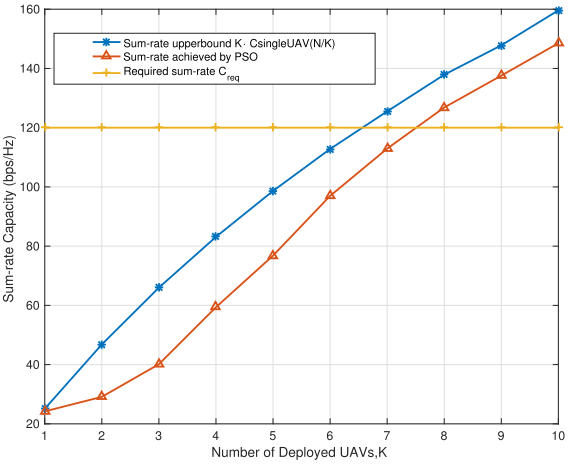

FIGURE 10. The sum-rate capacity as a function of the UAV number for $N = 120$ users.

Finally, we evaluate the performance improvement provided by the K-initialization schemes proposed in Sec. IV-B. Fig. 8 shows the single-UAV sum-rate $C_{\text{SingleUAV}}(N)$ given in (30) numerically derived by solving $\mathcal{P}4$ defined in (40).

By exploiting Fig. 8, we initialized K using "Init.K LBND" and "Init.K FixedPt" defined in (44) and (45), respectively, for $N = 40, 80, 120, 160$ users. Fig. 9 compares the initial K value derived from "Init.K LBND" and "Init.K FixedPt" as compared to the optimal K^* found by the proposed PSO scheme.

It is evident from Fig. 9, the "Init.K FixedPt" scheme has initialized K to a value much closer to the optimal K^* in all four test cases. As a result, only $(K^* - K_{\text{init}})$ PSO loops are required, which represents a significant reduction in computational complexity as compared to the case of setting $K_{init} = 1$.

An alternative way to demonstrate the effectiveness of the proposed initialization schemes is shown in Fig. 10. In this experiment, we consider a system of $N = 120$ users with the minimum required SINR of $\Gamma_0 = 0$ dB. As a result, the required sum-rate C_{req} is given by 120 bits-per-second-Hertz (bps/Hz) according to (29) as shown in the green

line with the cross markers in Fig. 10. Furthermore, the red curve with triangular markers indicates the sum-rate *actually* achieved by the proposed PSO scheme with the given number of UAVs. Clearly, the system cannot support C_{req} if K is small. Inspection of Fig. 10 suggests that the minimum of UAVs that can achieve $C_{\text{req}} = 120$ bps/Hz is $K^* = 8$. Finally, the blue curve with the asterisk markers shows the sum-rate $K \times C_{\text{SingleUAV}}(\frac{120}{K})$. According to (45), the "Init.K FixedPt" scheme sets $K_{\text{init}} = 7$ that is reasonably close to the optimal value $K^* = 8$.

VI. CONCLUSION

In this paper, we have developed a PSO-based UAV deployment scheme for interference-limited UAV-assisted wireless networks by optimizing three fundamental deployment issues, namely the minimum number of UAVs, their optimal deployment locations and the optimal transmit power allocation to satisfy a given SINR requirement. In order to derive the optimal locations and the optimal transmit power, we have adopted an SINR-balanced power allocation approach in updating each PSO generation. Furthermore, since the computational complexity of the proposed PSO-based scheme heavily depends on the initial estimate of the UAV number, two schemes have been proposed to accurately estimate the initial value of the UAV number by analyzing the network sum-rate capacity before the PSO iteration starts. In addition, we have proposed a K-means clustering-based initialization algorithm to initialize the UAV locations in the first PSO generation. Finally, a power fine-tuning scheme has been developed to further reduce the total transmit power. Extensive simulation results have confirmed the impressive performance of the proposed PSO-based schemes.

In our future work, we will consider relaxing some of the stringent assumptions employed in deriving the proposed schemes in this work. For instance, we will extend our work to the scenario where the user locations are not perfectly known and users are distributed in a larger area of different altitudes. In addition, we will consider more practical implementation constraints such as random wind gusts and network synchronization. As shown in [29], random wind gusts could lead to UE-UAV beam misalignment and subsequently, degrade the system performance. Furthermore, the synchronization issue among multiple UAVs can incur network capacity degradation [30]. We will explore more robust deployment schemes to combat such practical implementation challenges.

REFERENCES

[1] M. Mozaffari, W. Saad, M. Bennis, and M. Debbah, "Unmanned aerial vehicle with underlaid device-to-device communications: Performance and tradeoffs," *IEEE Trans. Wireless Commun.*, vol. 15, no. 6, pp. 3949–3963, Jun. 2016, doi: 10.1109/TWC.2016.2531652.

[2] Y. Zeng, R. Zhang, and T. J. Lim, "Wireless communications with unmanned aerial vehicles: Opportunities and challenges," *IEEE Commun. Mag.*, vol. 54, no. 5, pp. 36–42, May 2016, doi: 10.1109/MCOM.2016.7470933.

[3] Q. Wu, G. Y. Li, W. Chen, D. W. K. Ng, and R. Schober, "An overview of sustainable green 5G networks," *IEEE Wireless Commun.*, vol. 24, no. 4, pp. 72–80, Aug. 2017, doi: 10.1109/MWC.2017.1600343.

[4] H. Menouar, I. Guvenc, K. Akkaya, A. S. Uluagac, A. Kadri, and A. Tuncer, "UAV-enabled intelligent transportation systems for the smart city: Applications and challenges," *IEEE Commun. Mag.*, vol. 55, no. 3, pp. 22–28, Mar. 2017, doi: 10.1109/MCOM.2017.1600238CM.

[5] S. Sotheara, K. Aso, N. Aomi, and S. Shimamoto, "Effective data gathering and energy efficient communication protocol in wireless sensor networks employing UAV," in *Proc. IEEE Wireless Commun. Netw. Conf. (WCNC)*, Istanbul, Turkey, Apr. 2014, pp. 2342–2347, doi: 10.1109/WCNC.2014.6952715.

[6] T. A. Johansen, A. Zolich, T. Hansen, and A. J. Sorensen, "Unmanned aerial vehicle as communication relay for autonomous underwater vehicle—Field tests," in *Proc. IEEE Globecom Workshops (GC Wkshps)*, Austin, TX, USA, Dec. 2014, pp. 1469–1474, doi: 10.1109/GLOCOMW.2014.7063641.

[7] Y. Zeng, R. Zhang, and T. J. Lim, "Throughput maximization for UAV-enabled mobile relaying systems," *IEEE Trans. Commun.*, vol. 64, no. 12, pp. 4983–4996, Dec. 2016, doi: 10.1109/TCOMM.2016.2611512.

[8] A. Al-Hourani, S. Kandeepan, and S. Lardner, "Optimal LAP altitude for maximum coverage," *IEEE Wireless Commun. Lett.*, vol. 3, no. 6, pp. 569–572, Dec. 2014, doi: 10.1109/LWC.2014.2342736.

[9] M. Mozaffari, W. Saad, M. Bennis, and M. Debbah, "Efficient deployment of multiple unmanned aerial vehicles for optimal wireless coverage," *IEEE Commun. Lett.*, vol. 20, no. 8, pp. 1647–1650, Aug. 2016, doi: 10.1109/LCOMM.2016.2578312.

[10] A. Al-Hourani, S. Kandeepan, and A. Jamalipour, "Modeling air-to-ground path loss for low altitude platforms in urban environments," in *Proc. IEEE Global Commun. Conf.*, Austin, TX, USA, Dec. 2014, pp. 2898–2904, doi: 10.1109/GLOCOM.2014.7037248.

[11] L. Zhang and N. Ansari, "On the number and 3-D placement of in-band full-duplex enabled drone-mounted base-stations," *IEEE Wireless Commun. Lett.*, vol. 8, no. 1, pp. 221–224, Feb. 2019, doi: 10.1109/LWC.2018.2867501.

[12] H. Shakhatreh, A. Khreishah, A. Alsarhan, I. Khalil, A. Sawalmeh, and N. S. Othman, "Efficient 3D placement of a UAV using particle swarm optimization," in *Proc. 8th Int. Conf. Inf. Commun. Syst. (ICICS)*, Irbid, Jordan, Apr. 2017, pp. 258–263, doi: 10.1109/IACS.2017.7921981.

[13] A. Merwaday and I. Guvenc, "UAV assisted heterogeneous networks for public safety communications," in *Proc. IEEE Wireless Commun. Netw. Conf. Workshops (WCNCW)*, New Orleans, LA, USA, Mar. 2015, pp. 329–334, doi: 10.1109/WCNCW.2015.7122576.

[14] E. Bulut and I. Guevenc, "Trajectory optimization for cellular-connected UAVs with disconnectivity constraint," in *Proc. IEEE Int. Conf. Commun. Workshops (ICC Workshops)*, Kansas City, MO, USA, May 2018, pp. 1–6, doi: 10.1109/ICCW.2018.8403623.

[15] C. Yan, L. Fu, J. Zhang, and J. Wang, "A comprehensive survey on UAV communication channel modeling," *IEEE Access*, vol. 7, pp. 107769–107792, 2019, doi: 10.1109/ACCESS.2019.2933173.

[16] X. Cai, J. Rodriguez-Pineiro, X. Yin, N. Wang, B. Ai, G. F. Pedersen, and A. P. Yuste, "An empirical air-to-ground channel model based on passive measurements in LTE," *IEEE Trans. Veh. Technol.*, vol. 68, no. 2, pp. 1140–1154, Feb. 2019, doi: 10.1109/TVT.2018.2886961.

[17] Q. Wu, Y. Zeng, and R. Zhang, "Joint trajectory and communication design for multi-UAV enabled wireless networks," *IEEE Trans. Wireless Commun.*, vol. 17, no. 3, pp. 2109–2121, Mar. 2018, doi: 10.1109/TWC.2017.2789293.

[18] M. Mozaffari, W. Saad, M. Bennis, and M. Debbah, "Mobile unmanned aerial vehicles (UAVs) for energy-efficient Internet of Things communications," *IEEE Trans. Wireless Commun.*, vol. 16, no. 11, pp. 7574–7589, Nov. 2017, doi: 10.1109/TWC.2017.2751045.

[19] C.-T. Li, T.-Y. Wu, C.-L. Chen, C.-C. Lee, and C.-M. Chen, "An efficient user authentication and user anonymity scheme with provably security for IoT-based medical care system," *Sensors*, vol. 17, no. 7, p. 1482, 2017.

[20] E. T. Ceran, T. Erkilic, E. Uysal-Biyikoglu, T. Girici, and K. Leblebicioglu, "Optimal energy allocation policies for a high altitude flying wireless access point," *Trans. Emerg. Telecommun. Technol.*, vol. 28, no. 4, p. e3034, Apr. 2017.

[21] W. Liu, G. Niu, Q. Cao, M.-O. Pun, and J. Chen, "3-D placement of UAVs based on SIR-measured PSO algorithm," in *Proc. IEEE Globecom Workshops (GC Wkshps)*, Waikoloa, HI, USA, Dec. 2019, pp. 1–6, doi: 10.1109/GCWkshps45667.2019.9024696.

[22] J. Kennedy and R. Eberhart, "Particle swarm optimization," in *Proc. Int. Conf. Neural Netw. (ICNN)*, Perth, WA, Australia, vol. 4, Nov. 1995, pp. 1942–1948.

[23] Y. Shi and R. Eberhart, "A modified particle swarm optimizer," in *Proc. IEEE Int. Conf. Evol. Comput., IEEE World Congr. Comput. Intell.*, Anchorage, AK, USA, May 1998, pp. 69–73, doi: 10.1109/ICEC.1998.699146.
[24] P. Som and A. Chockalingam, "Damped belief propagation based near-optimal equalization of severely delay-spread UWB MIMO-ISI channels," in *Proc. IEEE Int. Conf. Commun.*, Cape Town, South Africa, May 2010, pp. 1–5, doi: 10.1109/ICC.2010.5502031.
[25] R. W. Nettleton and H. Alavi, "Power control for a spread spectrum cellular mobile radio system," in *Proc. 33rd IEEE Veh. Technol. Conf.*, Toronto, ON, Canada, May 1983, pp. 242–246, doi: 10.1109/VTC.1983.1623141.
[26] C. W. Tan, S. Friedland, and S. Low, "Nonnegative matrix inequalities and their application to nonconvex power control optimization," *SIAM J. Matrix Anal. Appl.*, vol. 32, no. 3, pp. 1030–1055, Jul. 2011.
[27] C. W. Tan, M. Chiang, and R. Srikant, "Maximizing sum rate and minimizing MSE on multiuser downlink: Optimality, fast algorithms and equivalence via max-min SINR," *IEEE Trans. Signal Process.*, vol. 59, no. 12, pp. 6127–6143, Dec. 2011, doi: 10.1109/TSP.2011.2165065.
[28] C. W. Tan, "Wireless network optimization by Perron-Frobenius theory," in *Proc. 48th Annu. Conf. Inf. Sci. Syst. (CISS)*, Princeton, NJ, USA, Mar. 2014, pp. 1–6, doi: 10.1109/CISS.2014.6814130.
[29] W. Yuan, C. Liu, F. Liu, S. Li, and D. W. K. Ng, "Learning-based predictive beamforming for UAV communications with jittering," *IEEE Wireless Commun. Lett.*, early access, Jul. 17, 2020, doi: 10.1109/LWC.2020.3009951.
[30] Y. Xiong, N. Wu, Y. Shen, and M. Z. Win, "Cooperative network synchronization: Asymptotic analysis," *IEEE Trans. Signal Process.*, vol. 66, no. 3, pp. 757–772, Feb. 2018, doi: 10.1109/TSP.2017.2759098.

WENTAO LIU received the bachelor's degree in information engineering from Xi'an Jiaotong University, China, in 2016, and the master's degree in telecommunications from the Hong Kong University of Science and Technology, China, in 2018. He is currently pursuing the Ph.D. degree with The Chinese University of Hong Kong, Shenzhen (CUHKSZ). His research interests include UAV-assisted wireless network design and machine learning.

GUANCHONG NIU received the bachelor's degree in physics from Jilin University, China, in 2014. He is currently pursuing the Ph.D. degree with The Chinese University of Hong Kong, Shenzhen (CUHKSZ). From January to March 2020, he was an Intern with Bell Labs, France, developing indoor localization systems. His current research interests include millimeter wave (mmWave) and multiple-input multiple-output (MIMO)systems for the next-generation wireless communications and robotics.

QI CAO received the bachelor's degree in electronic communication engineering from the University of Liverpool, in 2013, the M.S. degree in communications and signal processing from Imperial College, in 2014, and the Ph.D. degree from the School of Information and Control Engineering, China University of Mining and Technology, in 2018. He joined The Chinese University of Hong Kong, Shenzhen, as a Postdoctoral Research Associate, in 2019. His research interests include MIMO wireless communications and artificial intelligent (AI)-driven network optimization.

MAN-ON PUN (Senior Member, IEEE) received the B.Eng. degree in electronic engineering from The Chinese University of Hong Kong (CUHK), in 1996, the M.Eng. degree in computer science from the University of Tsukuba, Japan, in 1999, and the Ph.D. degree in electrical engineering from the University of Southern California (USC), Los Angeles, USA, in 2006.

From 2006 to 2008, he was a Postdoctoral Research Associate with Princeton University. He held research positions with Huawei, USA, Mitsubishi Electric Research Labs (MERL), Boston, and Sony, Tokyo, Japan. He is currently an Associate Professor with the School of Science and Engineering, The Chinese University of Hong Kong, Shenzhen (CUHKSZ). His research interests include the AI Internet of Things (AIoT) and applications of machine learning in communications and satellite remote sensing.

Dr. Pun has received best paper awards from the IEEE VTC'06 Fall, the IEEE ICC'08, and the IEEE Infocom'09. From 2010 to 2014, he served as an Associate Editor for the IEEE TRANSACTIONS ON WIRELESS COMMUNICATIONS. He is the Founding Chair of the IEEE Joint SPS-ComSoc Chapter, Shenzhen.

JUNTING CHEN worked with Prof. David Gesbert as a Postdoctoral Research Fellow with EURECOM, Sophia-Antipolis, France, from 2015 to 2016. From 2016 to 2018, he was a Postdoctoral Research Associate with Prof. Urbashi Mitra's Group, University of Southern California (USC), Los Angeles, CA, USA. Since 2019, he has been an Assistant Professor with the School of Science and Engineering, The Chinese University of Hong Kong, Shenzhen (CUHKSZ), China. He was an Active Contributor in several NFS projects, European Research Council (ERC) projects (SHARING and PERFUM) and industrial projects collaborating with Huawei Technologies, Paris, France. His research interest includes theories and solutions that range from 5G terrestrial communications to underwater communication networks.